M&C 2017 - International Conference on Mathematics & Computational Methods Applied to Nuclear Science & Engineering, Jeju, Korea, April 16-20, 2017, on USB (2017)

Solution Verification of CTF and CTF-R Using Isokinetic Advection Test Problems

Nathan Porter*, Maria Avramova*, Vincent Mousseau†

*North Carolina State University, 3140 Burlington Engineering Labs, 2500 Stinson Drive, Raleigh NC 27605
†Sandia National Laboratories, P.O. Box 5800, Albuquerque NM 87185-0748
nwporte2@ncsu.edu, mnavramo@ncsu.edu, vamouss@sandia.gov

Abstract - *This work performs a thorough code order verification study on COolant Boiling in Rod Arrays – Three Field (COBRA-TF) and the corresponding residual version. A very simple single-channel isokinetic advection problem is used with three different inlet conditions: constant, hyperbolic tangent, and cosine. The observed order of accuracy is shown to be one for all simulations, which is consistent with the formal order of accuracy. Small variations in the observed order can be attributed to iterative error in the solution algorithm, the influence of higher-order terms, secondary effects on the pressure and velocity, or possible mistakes in the coding or verification implementation. This work is one of the first code order verification studies to be documented for the current version of CTF, which is developed at North Carolina State University in cooperation with the Consortium for Advanced Simulation of Light Water Reactors.*

I. INTRODUCTION

COolant Boiling in Rod Arrays – Three Field (COBRA-TF) is a thermal hydraulic subchannel code designed for the analysis of Light Water Reactor (LWR) cores. Various versions of COBRA-TF exist throughout academia and industry. One version, rebranded as "CTF," is developed and maintained by the Reactor Dynamics and Fuel Modeling Group (RDFMG) at North Carolina State University (NCSU) [1]. CTF has recently been incorporated into the Consortium for Advanced Simulation of LWRs (CASL), which has led to rapid improvements in the code's capabilities, parallelization, performance, validation, and quality assurance.

The original version of COBRA-TF, designed at The Pacific Northwest National Laboratory (PNNL) in 1980 [2], was optimized to run on computers with limited capabilities. The code architecture and solution algorithms have remained essentially stagnant since then, so recent work has focused on modernizing the code. A residual formulation of COBRA-TF, called COBRA-IE, is used at The Bettis Atomic Power Laboratory [3, 4]. Similar work has commenced to introduce a residual formulation into the CASL version of CTF [5, 6]. An initial one dimensional residual formulation for single phase water with no source terms has been created and incorporated into the current version of CTF [7]. This option, which is nested inside CTF itself, is referred to as "CTF-R."

The residual formulation has a number of important benefits: flexibility to access and change the governing equations, the ability to discretize equations in different ways, ability to make the solution more implicit, the possibility of implementing a direct steady state solution, ability to build the pressure matrix or Jacobian in a variety of ways, the option of fully integrating solver packages into the solution algorithm because the numerical solution is separated from the physics, and potentially a quicker and more accurate solution.

Though CTF is a mature code that has been used throughout industry and academia, it lacks any formal code order verification studies. Similarly, CTF-R has no code verification studies because its development has just started. This work is intended to show that the underlying computer science and mathematical solution of these two codes are correctly implemented.

II. THEORY

This work will verify CTF-R and CTF through a comparison between formal and observed orders of accuracy. The governing equations are briefly outlined, then a test problem is selected for the code verification process. A modified equation analysis reveals the formal order of accuracy for this test problem. Finally, the convergence test procedure is outlined.

1. Governing Equations

The main version of CTF solves eight conservation equations, but only three of these have been implemented in CTF-R thus far. These are conservation of mass, momentum, and energy for single phase water in one dimension with no source terms.

$$\frac{\partial \rho}{\partial t} + \frac{\partial \rho u}{\partial x} = 0 \tag{1}$$

$$\frac{\partial u}{\partial t} + u\frac{\partial u}{\partial x} + \frac{1}{\rho}\frac{\partial P}{\partial x} = 0 \tag{2}$$

$$\frac{\partial \rho h}{\partial t} + \frac{\partial \rho h u}{\partial x} - \frac{\partial P}{\partial t} = 0 \tag{3}$$

CTF uses the nonconservative form of the momentum equation. Also of note is that a term in the energy equation, $u\,(\partial P/\partial x)$, is neglected. Pressure gradients are generally small, so this is deemed an appropriate approximation.

The source terms – friction, heat transfer, mixing, etc. – are disabled in the main version of CTF using multipliers that expose these models to user input. The gravity term in the momentum equation is disabled in a similar way. The equations in both codes are discretized over the same staggered mesh and they share a common input, so the two code options are expected to have the same solution.

2. Isokinetic Advection Test Problem

An isokinetic advection test problem is designed to verify both the main version of CTF and the new residual formulation. The initial conditions are designed such that the pressure and velocity are constant throughout domain, then the inlet conditions are allowed to advect through the channel at the constant velocity, u.

With a constant velocity and pressure, the conservation equations simplify significantly. The momentum equation becomes trivial, and both the mass and energy equations take the same form.

$$\frac{\partial \rho}{\partial t} + u\frac{\partial \rho}{\partial x} = 0 \tag{4}$$

$$\frac{\partial \rho h}{\partial t} + u\frac{\partial \rho h}{\partial x} = 0 \tag{5}$$

Density and enthalpy are governed by the same advective properties for this simulation, so either can be examined for convergence. Enthalpy is selected as the quantity of interest because it is directly used as the boundary condition in both versions of CTF. This will eliminate error due to the nonlinear equation of state from the convergence procedure.

The parameters which define the problem are outlined in Table I. The conditions approximate a subchannel with reactor geometry at near standard pressure and temperature. There is a maximum change in temperature of $2°C$. The water is subcooled throughout all simulations. The problem was designed such that the inlet condition will advect to the outlet of the channel in about ten seconds. The time of interest for all simulations is when the inlet condition has advected half way through the channel.

TABLE I: Problem Parameters for Isokinetic Advection

Parameter	Symbol	Value	Units
Channel Length	L	0.5	m
Flow Area	A	0.0001	m^2
Wetted Perimeter	P_w	0.040	m
Pressure	P	1.00	bar
Initial Temperature	T_o	40	$°C$
Initial Enthalpy	h_o	167.6	kJ/kg
Initial Density	ρ_o	992.22	kg/m^3
Initial Flow Rate	$\dot{m}_o$	0.005	kg/s
Velocity	u	0.05039	m/s
"Inlet" Temperature	T_{in}	38	$°C$
"Inlet" Enthalpy	h_{in}	159.22	kJ/kg
"Inlet" Density	ρ_{in}	992.90	kg/m^3
"Inlet" Flow Rate	$\dot{m}_{in}$	0.05004	kg/s
Hyperbolic Tangent Width	l	0.05	m
Hyperbolic Tangent Offset	τ	5.0	s
Cosine Wave Period	p	L/u	s

Three inlet condition types are chosen: square wave, hyperbolic tangent, and cosine wave. The square wave is selected for its simplicity; both the inlet condition and the initial condition are constant. For the square wave, solution of Equation 4 or 5 is a step function.

$$h_{sq} = \begin{cases} h_o, & ut \le x \\ h_{in}, & ut > x \end{cases} \tag{6}$$

The second inlet condition type is the hyperbolic tangent. This condition is selected because, like the square wave condition, it is smooth with the initial condition, but lacks the discontinuity at the wave location.

$$h_{tanh} = \begin{cases} h_o, & ut \le x \\ \frac{1}{2}\left[(h_o + h_{in}) - (h_o - h_{in})\tanh\left(\frac{u(t-\tau)-x}{l}\right)\right], & ut > x \end{cases} \tag{7}$$

A characteristic length, l, determines how wide the hyperbolic tangent is. The constant τ is necessary to shift the wave left, which allows the inlet and initial condition to be approximately equal at the beginning of the simulation. When using the hyperbolic tangent inlet condition, the time of interest for all simulations will be at five seconds plus the offset.

The final inlet condition type is a cosine wave. The cosine is selected such that it is continuous with the initial condition.

$$h_{cos} = \begin{cases} h_o, & ut \le x \\ \frac{1}{2}\left[(h_o + h_{in}) + (h_o - h_{in})\cos\left(\frac{2\pi}{p}\left(t - \frac{x}{u}\right)\right)\right], & ut > x \end{cases} \tag{8}$$

The cosine period, p, is equal to the channel length divided by the velocity, u. Therefore, the wavelength is equal to the channel length.

To ensure that all derivatives of the solution are smooth, the initial condition should also be a cosine shape. CTF input does not allow for a nonuniform initial condition, so there may be a small amount of error that originates from the discontinuous second derivative at the wave location.

3. Modified Equation Analysis

Modified Equation Analysis [8] is used to define the formal order of accuracy of discretized equations by estimating the truncation error of a given discretization scheme. The analysis starts with a discretized form of Equation 4 with a constant positive velocity and upwinded advection term.

$$\frac{\rho_i^{n+1} - \rho_i^n}{\Delta t} + u\frac{\rho_i^n - \rho_{i-1}^n}{\Delta x} = 0 \tag{9}$$

Second order Taylor series expansions about i and n are used to approximate ρ_i^{n+1} and ρ_{i-1}^n.

$$\rho_i^{n+1} = \rho_i^n + \left.\frac{\partial \rho}{\partial t}\right|_i^n \Delta t + \frac{1}{2}\left.\frac{\partial^2 \rho}{\partial t^2}\right|_i^n \Delta t^2 + O\left(\Delta t^3\right) \tag{10}$$

$$\rho_{i-1}^n = \rho_i^n - \left.\frac{\partial \rho}{\partial x}\right|_i^n \Delta x + \frac{1}{2}\left.\frac{\partial^2 \rho}{\partial x^2}\right|_i^n \Delta x^2 + O\left(\Delta x^3\right) \tag{11}$$

Equations 9, 10, and 11 are combined and rearranged with the original conservation equation on the left and the error terms on the right.

$$\frac{\partial \rho}{\partial t} + u\frac{\partial \rho}{\partial x} = \left[\frac{u}{2}\frac{\partial^2 \rho}{\partial x^2}\right]\Delta x - \left[\frac{1}{2}\frac{\partial^2 \rho}{\partial t^2}\right]\Delta t \tag{12}$$

This equation defines the general behavior of error in CTF. The formal order of accuracy is first order in both space and time when the higher order terms are sufficiently small that they can be neglected. Similar results can be derived using Equation 5.

4. Convergence Study Procedure

Convergence tests are performed by running identical simulations with different temporal or spatial meshes. Three metrics are used to assess the change between two successively refined simulations.

$$||h||_1 = \sum_i \left|h_{i,fine} - h_{i,coarse}\right| \tag{13}$$

$$||h||_2 = \sqrt{\sum_i \left(h_{i,fine} - h_{i,coarse}\right)^2} \tag{14}$$

$$||h||_\infty = \max \left|h_{i,fine} - h_{i,coarse}\right| \tag{15}$$

The observed order of accuracy p is determined by finding a line of best fit with the exponential form, $||h|| = cx^p$. The coefficient of determination, R^2, demonstrates how closely the line approximates the results.

Three types of convergence studies are considered in this work. Temporal and spatial convergence studies are used to demonstrate correct scaling with Δt and Δx, respectively. Then, both the spatial and temporal meshes are refined at the same rate to demonstrate the behavior for normal code usage.

The selection of suitable Δx and Δt combinations is an important part of the convergence study process. The solution must be stable, while also having a feasible computational time. Equation 12 can be used to derive the Courant Fourier Limit (CFL), which directly determines the stability of the single-phase solutions in this work.

Equation 1 is used to find a relationship between the second derivative with respect to space and the second derivative with respect to time, $\left(\partial^2\rho/\partial t^2\right) = u^2\left(\partial^2\rho/\partial x^2\right)$. This result is combined with Equation 12 to derive a stability criterion.

$$\frac{\partial \rho}{\partial t} + u\frac{\partial \rho}{\partial x} = \frac{u\Delta x}{2}\frac{\partial^2 \rho}{\partial x^2}\left(1 - \text{CFL}\right) \tag{16}$$

The CFL is defined as $u\Delta t/\Delta x$. When the CFL is less than one, the error term causes diffusion. When the CFL number is larger than one, the diffusion term becomes an anti-diffusion operator and the solution is unstable. The CFL is below 1.0 for all simulations in this work.

III. RESULTS

The results from convergence tests of the isokinetic advection problem using all three inlet conditions are given in this section.

1. Square Wave Advection

Typical enthalpies from the simulation of the square wave advection problem are shown in Figure 1a. The results are compared to Equation 6, which is represented as dashed lines in the figure. The difference between the analytical and code results are shown in Figure 1b. CTF and CTF-R have such similar results that they cannot be distinguished graphically, so only the residual formulation results are shown. CTF predicts the solution well, with characteristic diffusion around the discontinuity. This is the expected result and demonstrates that the test problem is set up correctly.

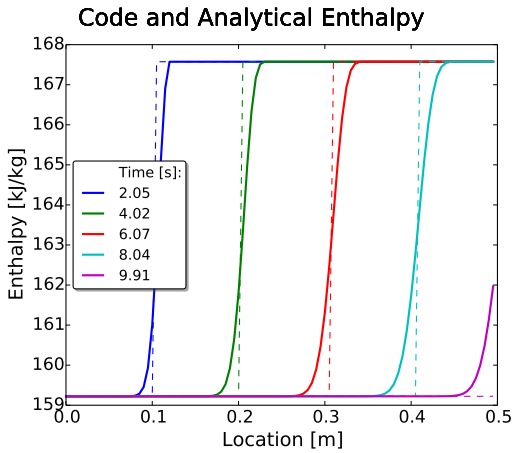

(a) Code results are solid, corresponding results from Equation 6 are dashed

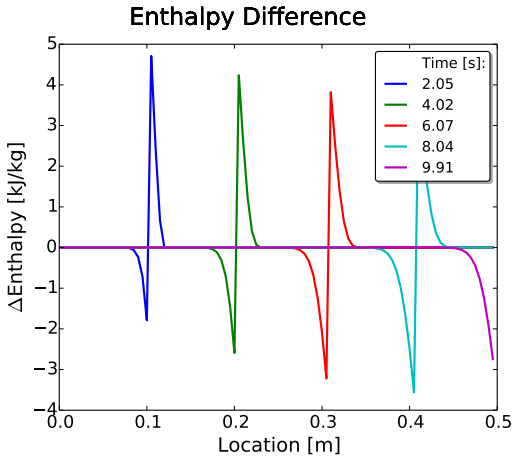

(b) Difference between code and analytical results ($h_{sq} - h_{code}$)

Fig. 1: Example code run for square wave advection with $\Delta x = 0.05$ m, $\Delta t = 0.0893$ s, and CFL = 0.9

The results from a temporal order of accuracy study are shown in Figure 2. All three norm results are shown for each of the code versions along with the lines of best fit for each data set and their corresponding R^2 values. The resulting order of accuracy is essentially one for both codes.

2. Hyperbolic Tangent Advection

Results for the hyperbolic tangent inlet condition are shown in Figure 3. Similar to the square wave results, Figure 3a shows the code results and analytical solution, and Figure 3b is the difference between the two. The offset of the wave, τ, is sufficiently large that the solution is smooth. The error follows the wave location and again shows the expected diffusion behavior. These results indicate that the problem is set up correctly.

Temporal, spatial, and constant CFL convergence studies were performed with the hyperbolic tangent condition and the results are shown in Figures 4a, 4b, and 4c, respectively. All three studies have observed orders of accuracy approximately equal to one.

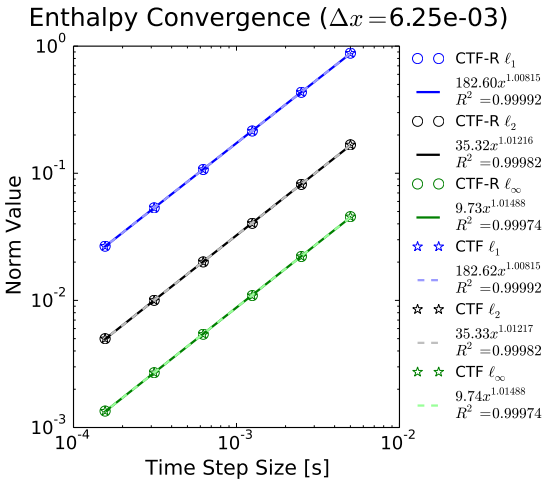

Fig. 2: Square wave advection temporal convergence results

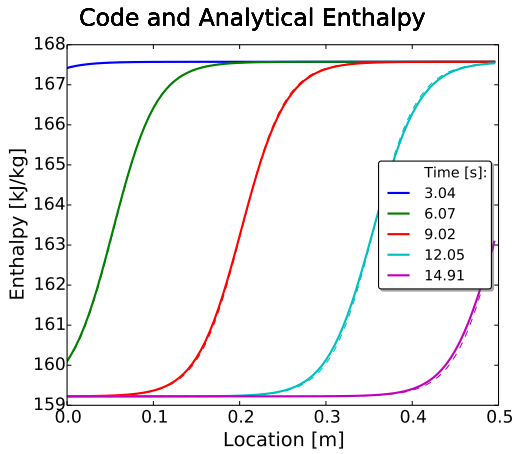

(a) Code results are solid, corresponding results from Equation 7 are dashed

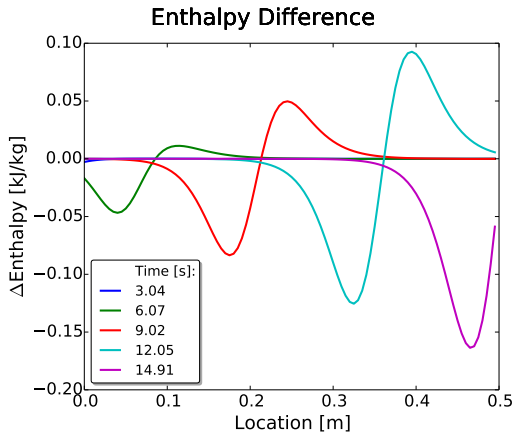

(b) Difference between code and analytical results ($h_{tanh} - h_{code}$)

Fig. 3: Example code run for hyperbolic tangent advection with Δx = 0.05 m, Δt = 0.0893 s, and CFL = 0.9

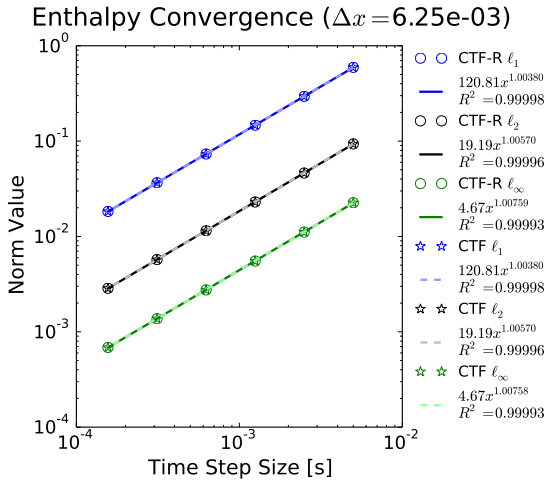

(a) Temporal convergence

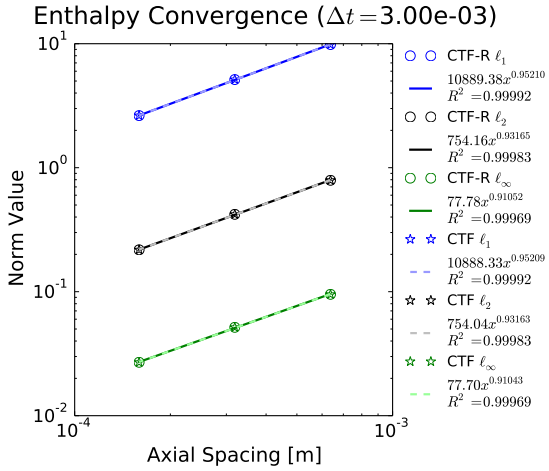

(b) Spatial convergence

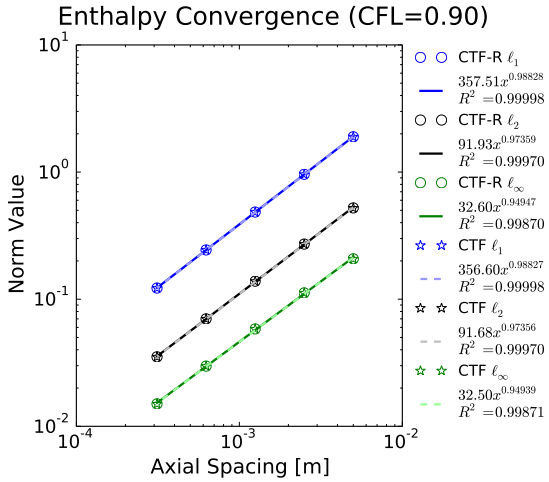

(c) Constant CFL convergence

Fig. 4: Convergence study results using hyperbolic tangent inlet condition

3. Cosine Wave Advection

Typical results for the cosine advection problem are shown in Figure 5a, and the difference between the code and analytical solution are shown in Figure 5b. Again, the CTF results are solid and the analytical solution is dashed. The code results match well with the analytical solution.

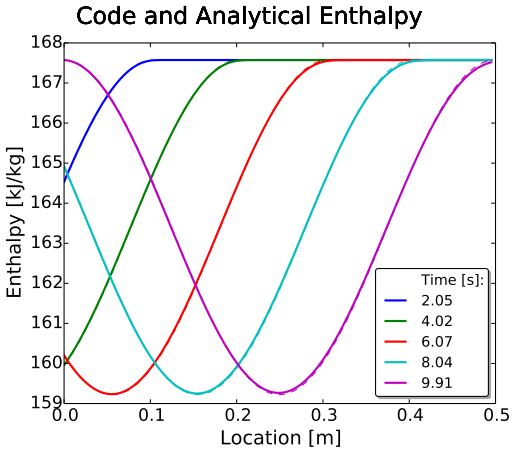

(a) Code results are solid, corresponding results from Equation 8 are dashed

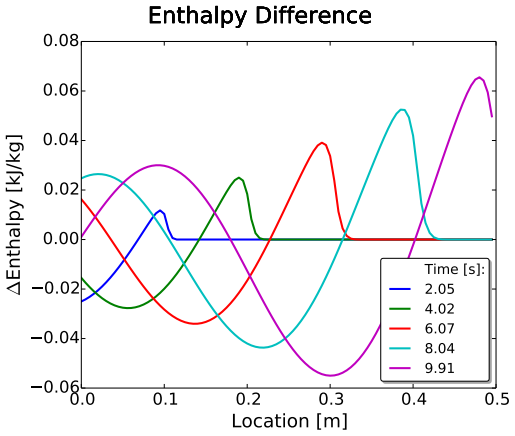

(b) Difference between code and analytical results ($h_{cos} - h_{code}$)

Fig. 5: Example code run for cosine wave advection with Δx = 0.05 m, Δt = 0.0893 s, and CFL = 0.9

Finally, the cosine wave isokinetic advection test problem is used to perform three convergence studies. The results are shown in Figures 6a, 6b, and 6c. All observed orders of accuracy are near unity, which demonstrates that the codes are first order in both space and time.

IV. CONCLUSIONS

All observed orders of accuracy using the L_2 norm are summarized in Table II. All values are between 0.9 and 1.1. Small variations in the observed order of accuracy can originate from a variety of sources, such as iterative error, small coding mistakes, incorrect verification test implementation, and the influence of higher order terms that were neglected during the modified equation analysis.

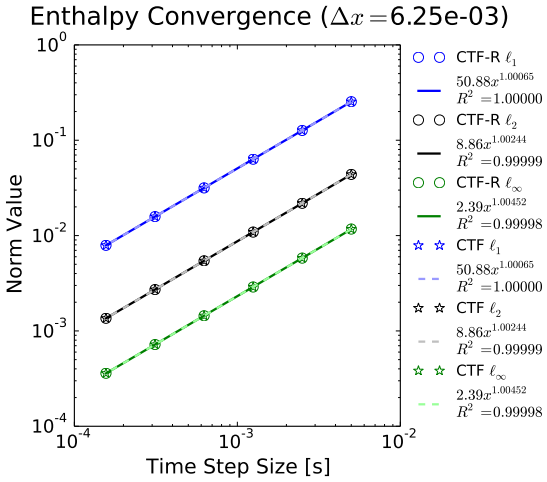

(a) Temporal convergence

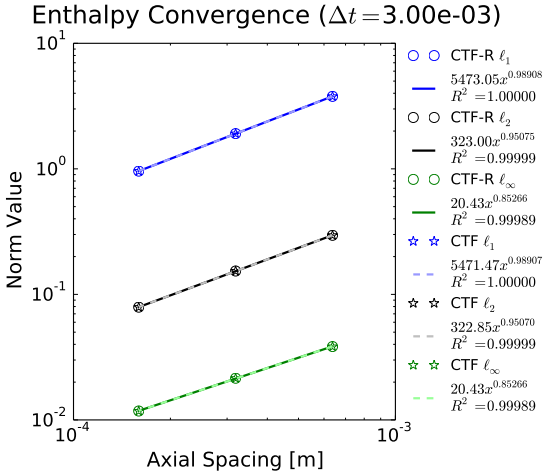

(b) Spatial convergence

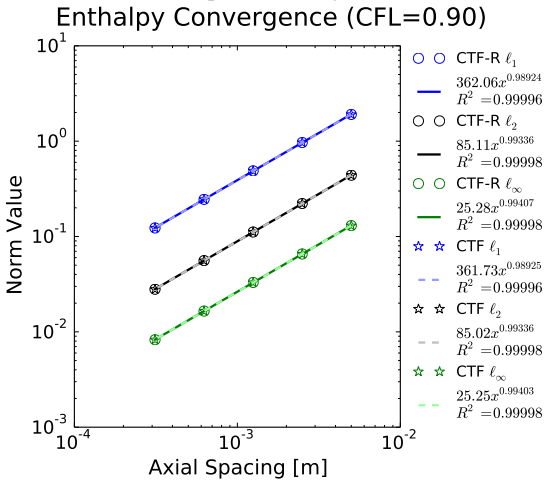

(c) Constant CFL convergence

Fig. 6: Convergence study results using cosine wave isokinetic advection

TABLE II: Summary of observed orders of accuracy

Inlet	Type	CTF-R	CTF
square	Δt	1.01216	1.01217
tanh	Δt	1.00570	1.00570
	Δx	0.93165	0.93163
	CFL	0.97359	0.97356
cos	Δt	1.00244	1.00244
	Δx	0.95075	0.95070
	CFL	0.99336	0.99336

The run times for all simulations are shown in Figures 7a, 7b, and 7c for the temporal, spatial, and constant CFL convergence studies, respectively. Note that the spatial convergence study, Figure 7b, scales very poorly with mesh size for CTF-R. This is due to the high computational cost of solving the full Jacobian. The poor scaling of Δx with computational cost, compounded with the inverse relationship between CFL and Δx, causes computational and stability limitations to force the simulations outside of the asymptotic range. As such, the observed orders of accuracy for spatial convergence are the furthest from one.

The analytical solution completely eliminates the momentum equation, but this cannot be done in practice. As a result, vary small variations in the momentum equation cause secondary effects on the pressure and velocity for all simulations. The secondary effects on pressure and velocity for the square wave inlet condition are shown in Figures 8a and 8b, respectively. The secondary effects follow the location of the wave and are due to the nonlinearity of the equation of state. Note that the scales of the figures are small, so the secondary effects are not significant to the convergence studies.

It has been shown that the formal order of accuracy and the observed order match for both CTF and CTF-R when using an isokinetic advection test problem. Small variations can be attributed to a variety of sources, but the differences are sufficiently small to conclude that the code is overall first order. Therefore, the solution algorithms for both codes have been implemented correctly and give correct results.

The isokinetic advection problem was designed to test the mass and energy conservation equations. Therefore, future code verification work will focus on the momentum equation. In addition, the residual formulation is currently in its infancy and must be expanded in a number of ways: adding closure relations, the conduction solution, transverse momentum equation, and the additional gas and droplet phases. Work will also focus on reducing the computational cost of the Jacobian solution. Overall, this work is an indication that CTF-R is being developed correctly and these test problems will be used to ensure that the code does not regress during further development.

V. ACKNOWLEDGMENTS

This work was partially funded by CASL (www.casl.gov), an Energy Innovation Hub (www.energy.gov/hubs) for Modeling and Simulation of Nuclear Reactors under the United States Department of Energy.

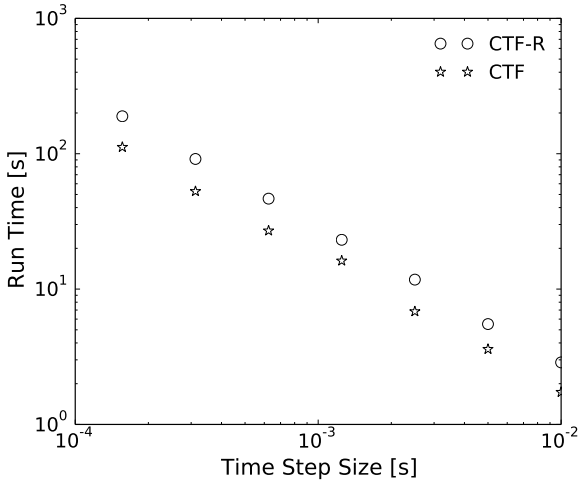

(a) Constant Δx run times

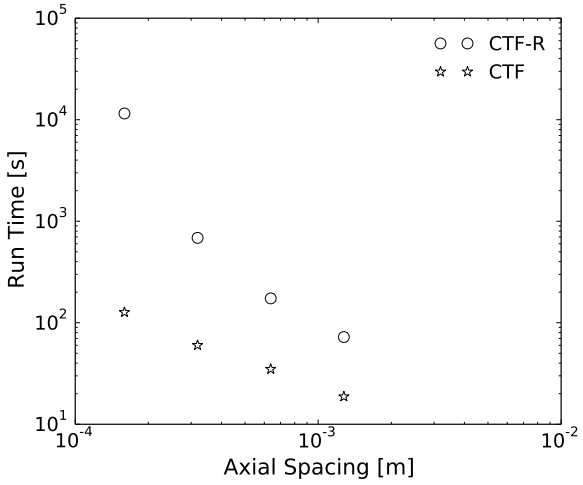

(b) Constant Δt run times

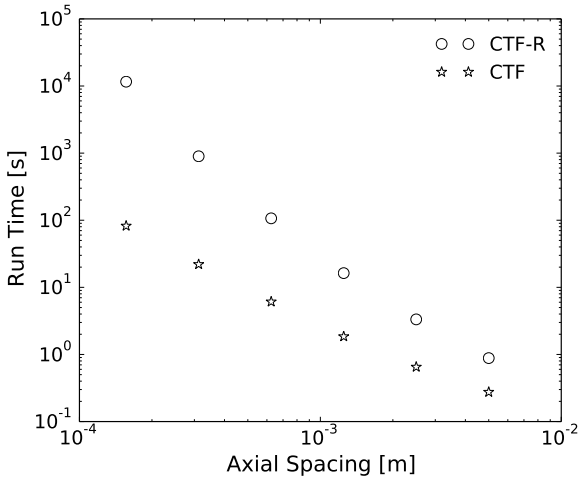

(c) Constant CFL run times

Fig. 7: Simulation time for hyperbolic tangent problems

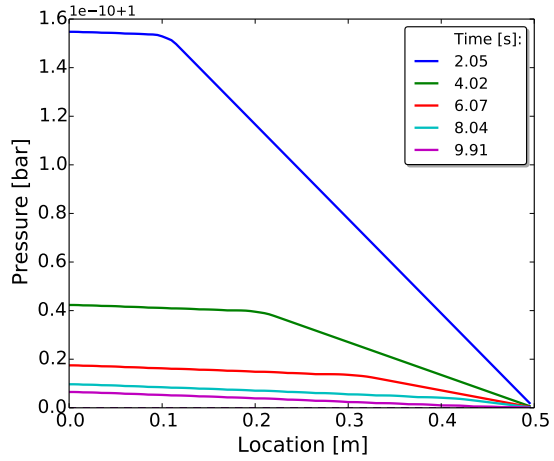

(a) Pressure effects for square wave inlet condition

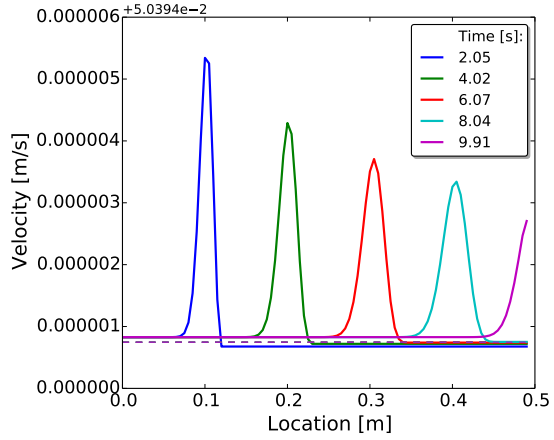

(b) Velocity effects for square wave inlet condition

Fig. 8: Secondary effects with $\Delta x = 0.05$ m, $\Delta t = 0.0893$ s, and CFL = 0.9

REFERENCES

1. R. K. SALKO and M. N. AVRAMOVA, *CTF Theory Manual*, North Carolina State University (September 2016).
2. M. J. THURGOOD ET AL., "COBRA/TRAC: A Thermal-Hydraulics Code for Transient Analysis of Nuclear Reactor Vessels and Primary Coolant Systems," Tech. Rep. NUREG/CR-3046, PNL-4385, US Nuclear Regulatory Commission (1983).
3. C. J. BURNS and D. L. AUMILLER, "COBRA-IE Evaluation by Simulation of the NUPEC BWR Full-Size Fine-Mesh Bundle Test (BFBT)," Tech. Rep. B-T-3653, Bechtel Bettis, Inc. (2007).
4. L. J. LLOYD, *Development of Spatially-Selective, Nonlinear Refinement Algorithm for Thermal-Hydraulic Safety Analysis*, Ph.D. thesis, University of Wisconsin–Madison (2014).
5. C. A. DANCES and V. A. MOUSSEAU, "Preliminary Residual Formulation of COBRA-TF," in D. P. KOURI and M. L. PARKS, editors, "Center for Computing Reasearch Summer Proceedings," Sandia National Laboratories (December 2014), SAND2015-3829O, pp. 105–124.
6. C. A. DANCES, *Initial Residual Formulation of CTF*, Master's thesis, Pennsylvania State University (May 2015).
7. N. W. PORTER, V. A. MOUSSEAU, and M. N. AVRAMOVA, "Initial Residual Formulation of CTF for One Dimensional, Single Phase Flow," Tech. Rep. U-2016-1183-000, CASL (August 2016).
8. C. W. HIRT, "Heuristic Stability Theory for Finite-Difference Equations," *Journal of Computational Physics*, **2**, 339–355 (1968).